Robust LMI-Based Active Fault Tolerant Pitch Control of a Wind Turbine Using a Fuzzy Model

A. Bakhshi, A. Alfi

Faculty of Electrical and Robotic Engineering, Shahrood University of Technology, Shahrood, 36199-95161, Iran, (e-mail: a_alfi@shahroodut.ac.ir)

Abstract: This article seeks to investigate a robust active fault-tolerant control strategy for a wind turbine system in the presence of actuator and sensor fault. The state-space representation of the system was formulated by the Takagi-Sugeno fuzzy model and then, a disturbance rejection technique is used to eliminate the wind perturbation. To guarantee the robust behavior of the system, the control signal is reconfigured through adding a robust term. By using the Lyapunov method, some criteria, which are expressed in the form of linear matrix inequalities (LMIs), are provided for asymptotic stability of the estimated error. Finally, the main results were confirmed by numerical simulations of a 1 MW wind turbine.

Keywords: Fault-tolerant control; LMI; Pitch control; Takagi-Sugeno model; Robust behavior; Wind turbine

1. INTRODUCTION

The traditional fossil and nuclear energy threaten the natural environment. Wind energy is regarded as one of the well-known renewable energy to reduce the consumption of fossil and nuclear fuels. Considering the probability of fault occurrence in industrial systems, maintaining the system performance under distinct faults is essential to reduce the electrical energy production cost. The combination of fault diagnosis and identification (FDI) with the control reconfiguration (CR) is called fault-tolerant control (FTC). Generally, different types of faults, such as pitch and hydraulic system faults (Odgaard and Johnson, 2013), may be occurred in the wind turbines. In fact, the occurrence of such faults in a wind turbine under the full load area can significantly jeopardize the system's performance and even lead to poor stability of the pitch control system. So far, several techniques of FDI and FTC schemes have been proposed for horizontal wind turbines (Saha and Singh, 2019). However, a turbine has different dynamics and control inputs, including the generator torque and pitch angle, should be designed to achieve the system requirements separately. Different regions are determined to be subjected to the values of rotor speed and generator torque. Concerning the pitch control region, the rotor speed is greater than the set-point value and the generator torque has its maximum value. The pitch control and the torque control are two separate control strategies used in the wind turbine, because of the dynamic variations of the system nature (Burton et al., 2011). (Nourdine et al., 2010) introduced a pitch control for each blade with a linear quadratic Gaussian controller and load reduction. (Taher et al., 2013) studied an optimization problem for designing a bank of linear quadratic regulator (LQR) controllers in a gain scheduling strategy. (Habibi et al., 2019) developed a model based on FDI and FTC techniques in a wind turbine. (Odgaard et al., 2013) proposed a benchmark model for accommodation and fault detection. By solving bilinear matrix inequalities, (Sloth et al., 2011) reviewed both passive and active FTC strategies in the full load region for the pitch system. (Blesa et al., 2014) applied FDI and FTC techniques on a wind turbine to identify sensor and actuator faults, by using interval observers and virtual sensors/actuators, respectively. Moreover, the batch least-squares technique was used for the faults estimation. (Azizi et al., 2019) employed an adaptive output-feedback sliding mode technique to construct an FTC of a wind turbine. (Ettouil et al., 2018) developed a synergetic FTC control for pitch system by applying an adaptive observer. Using automatic signal correction, an active FTC scheme based on fault detection and diagnosis (FDD) was proposed to control wind turbine pitch angle in the presence of uncertainties and measurement noise (Badihi et al., 2020).

In practice, since the exact value of effective wind speed is not available, the wind speed has been estimated using the Kalman filter. Further, a nonlinear state-feedback controller was designed to achieve the desired performance. (Soltani et al., 2013) conducted a comprehensive study on distinct techniques for wind speed estimation. (Shi and Patton, 2015) estimated the system states and the fault signals by an extended state observer in a linear parameter-varying system, although the pole-placement and H∞ optimization ensured the performance requirements and the overall closed-loop robustness. (Casau et al., 2015) used a set-valued observer for fault detection of an uncertain linear time-varying system against exogenous disturbances, measurement noise and model uncertainty. Furthermore, both active and passive FTCs were applied for the system configuration. (Simani and Castaldi, 2014) introduced a nonlinear geometric approach based adaptive filters for fault estimation and then, analyzed the stability of the system under different faults. (Li et al., 2020) designed a time-varying estimator using an active FTC strategy to eliminate the effect of a sensor fault. The stability analysis of the estimator and model predictive controller were investigated using the LMI technique. It is worth noting that the Lyapunov-based method is a common technique for stability analysis (Haidegger et al., 2011a; Haidegger et al.,

2011b). (Ghanbarpour et al., 2020) presented a robust sliding mode observer design for sensor faults, along with online linearization. (Xiahou et al., 2020) considered the stator and rotor current sensor faults occurred in a doubly-fed induction generator. Sensor faults were tolerated by a reconfiguration structure, considering vector control scheme.

The fuzzy-based fault controller is another technique, which has been highly considered in recent years (Obe and Dumitrache, 2012). (Badihi et al., 2014) designed a fuzzy gain scheduling algorithm with a proportional-integral controller under measurement noise, wind turbulence, and different faults. (Georg and Schulte, 2014) implemented a sector non-linearity approach with Takagi-Sugeno Sliding Mode Observer (TS SMO) on a non-affine complex wind turbine system. Besides, the existence of sliding motion has been proved through the reachability condition. (Schulte and Gauterin, 2015) employed the fault reconstruction strategy to modify inputs as virtual actuators in a hydrostatic wind turbine, in addition to applying the TS SMO scheme to achieve FDI and FTC. To the best of our knowledge, no research has been conducted on the fault-tolerant control strategy in the presence of disturbance in the field of wind turbines. Therefore, the present study aims to propose a structure to solve the problem of fault-tolerant control in the presence of disturbance for a wind turbine with complex nonlinear dynamics. To this aim, a robust active FTC (RFTC) is investigated for pitch control under the full load operation against disturbance and actuator faults. The contributions of the current research are listed below:

i) A new robust fault-tolerant control (RFTC) is developed for a nonlinear WT model. The simplicity of design, robust behaviour in the presence of disturbance and faults, and good response are among the prominent properties of the proposed control method.
ii) The WT is modeled as a set of Takagi-Sugeno (TS) fuzzy models to estimate the system's nonlinearities. Furthermore, sufficient conditions are derived to stabilize the system in the form of linear matrix inequalities (LMIs).
iii) An extended observer is designed to estimate both the system states and faults simultaneously.
iv) Stability analysis of the overall system, including the observer and the FTC controller, is given using the Lyapunov method.

It should be noted that the key novelty of this article consists of the closed-loop stability analysis of a nonlinear system in a convergence region under disturbance, sensor, and actuator faults.

The rest of the paper is organized as follows. Section 2 gives the problem description. Section 3 explains the fault-tolerant scheme with the disturbance rejection problem. Section 4 evaluates the performance of the proposed control using numerical simulations, which consist of actuator faults, sensor faults and comparison scenario. Eventually, Section 5 provides the conclusion made in this research.

2. PROBLEM FORMULATION

This paper addresses the problem of pitch control under the full load operation for a wind turbine. The nonlinear dynamical equations of the desired system have been given by (Kühne et al., 2018).

$$\begin{cases} \dot{\theta}_s(t) = \omega_r(t) - \omega_g(t) \\ \dot{\omega}_r(t) = -\dfrac{\overline{K}_s}{J_r}\theta_s - \dfrac{\overline{B}_s}{J_r}\omega_r + \dfrac{\overline{B}_s}{J_r}\omega_g + \dfrac{\overline{T}_r}{J_r} \\ \dot{\omega}_g(t) = \dfrac{\overline{K}_s}{J_g}\theta_s - \dfrac{\overline{B}_s}{J_g}\omega_r - \dfrac{\overline{B}_s}{J_r}\omega_g - \dfrac{\overline{T}_g}{J_g} \\ \dot{\beta}(t) = -\dfrac{1}{\tau}\beta + \dfrac{1}{\tau}\beta_d \end{cases} \quad (1)$$

where θ_s, ω_r, ω_g and β are shaft torsion angle, rotor angular velocity, generator angular velocity, and pitch angle respectively. Table 1 lists the other parameters of the wind turbine.

The aerodynamic torque is determined by the following relation:

$$\overline{T}_r = \frac{1}{2\lambda}\rho\pi R^3 C_P(\lambda,\beta)\upsilon^2 \quad (2)$$

where C_P (λ, β) represents the power coefficient, v indicates the wind speed, and λ shows the blade tip speed ratio, which is defined as follows:

$$\lambda = \frac{R\omega_r}{\upsilon} \quad (3)$$

T_r can be linearized as follows:

$$\overline{T}_r = T_{r\upsilon}\upsilon + T_{r\beta}\beta \quad (4)$$

where

$$T_{r\nu} = \frac{d\overline{T}_r}{d\upsilon}\Big|(\upsilon^*,\beta^*) \qquad T_{r\beta} = \frac{d\overline{T}_r}{d\beta}\Big|(\upsilon^*,\beta^*) \quad (5)$$

The term C_P (λ, β) is computed by using a look-up table. There are several mathematical estimations to approximate the coefficient (for example, refer to (Kamal et al., 2012)). We consider the generator torque $\overline{T}_g$ as a function of generator speed, although its reference is given by the following relation:

$$\overline{T}_g = \overline{B}_g\omega_g - T_{g,ref} \quad (6)$$

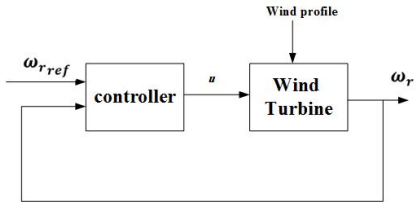

Fig. 1. Base-line control structure for wind turbine.

In this section, a set of locally linear models proposed by Takagi and Sugeno are constructed for estimating the original nonlinear dynamical system (Tanaka and Wang, 2003). The fuzzy model is expanded by IF-THEN rules. It has been proven

that this fuzzy model can approximate the wide class of nonlinear smooth systems with the desired precision. We consider a TS fuzzy model with fault and disturbance inputs, in which the state-space realization of an i^{th} rule is described as follows:

Rule *i*

IF

$$\gamma_1(x,u) \ \ is \ \ \psi_{i1} \ \ \ and ... and \ \ \gamma_p(x,u) \ \ is \ \ \psi_{ip} \tag{7}$$

Then

$$\begin{cases} \dot{x}(t) = A_i x(t) + Bu(t) + B_{\upsilon_i}\upsilon(t) + B_f f_1(t) \\ y(t) = Cx(t) + D_f f_2(t) \end{cases}$$

where $i = 1, \ldots, n$, and n represents the number of IF-THEN rules, $\gamma(x,u) = [\gamma_1(x,u), \ldots \gamma_p(x,u)]$ indicates the premise variables, and $\psi_{ij}(j = 1, .., p)$ is fuzzy sets. The membership functions of the fuzzy system are considered triangular, which are depicted in Fig. 2. By representing the states as

$$x = (\theta_s, \omega_r, \omega_g, \beta)^T \tag{8}$$

the state-space representation is expressed as follows:

$$A = \begin{bmatrix} 0 & \frac{1}{\bar{J}_r} & \frac{-1}{\bar{J}_r} & 0 \\ -\frac{\bar{K}_s}{\bar{J}_r} & -\frac{\bar{B}_s}{\bar{J}_r} & \frac{\bar{B}_s}{\bar{J}_r} & -\frac{T_{rB}}{\bar{J}_r} \\ \frac{\bar{K}_s}{\bar{J}_g} & \frac{\bar{B}_s}{\bar{J}_g} & -\frac{\bar{B}_s + \bar{B}_g}{\bar{J}_g} & 0 \\ 0 & 0 & 0 & -\frac{1}{\tau} \end{bmatrix}, \ B = \begin{bmatrix} 0 & 0 \\ 0 & 0 \\ 0 & \frac{1}{\bar{J}_g} \\ \frac{1}{\tau} & 0 \end{bmatrix}$$

$$B_\upsilon = \begin{bmatrix} 0 \\ \frac{T_{r\upsilon}}{\bar{J}_r} \\ 0 \\ 0 \end{bmatrix}, \ C^T = \begin{bmatrix} 0 \\ 1 \\ 0 \\ 0 \end{bmatrix} \tag{9}$$

Fig. 1. shows the base-line control strategy. Considering fault, we add an estimator block to the control configuration. Fig. 3 demonstrates the structure of the FTC system.

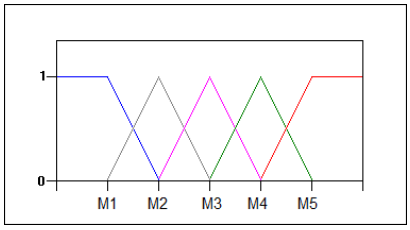

Fig. 2. Membership function of TS fuzzy system.

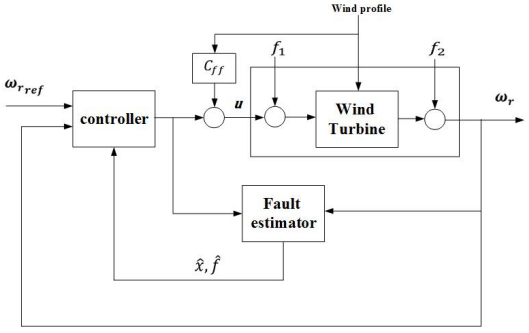

Fig. 3. FTC diagram for wind turbine.

3. FAULT TOLERANT CONTROLLER DESIGN WITH DISTURBANCE REJECTION

In general, different techniques are available in the FTC, due to the system requirements. In this paper, fault estimation is augmented with a base-line controller for designing an FTC scheme. Accordingly, an unknown input observer is designed to estimate the system states and the fault effects. The FTC rule can be achieved by a compensating term:

$$u = \sum_{i=1}^{n} \gamma_i(z(x,u)) \left(u_{base\,i} + u_{cri} + u_{FTC} \right) \tag{12}$$

where u_{FTC} and u_{cr} are the fault compensation and the disturbance rejection parts, respectively. The general block diagram of the TS fuzzy controller is shown in Fig. 4.

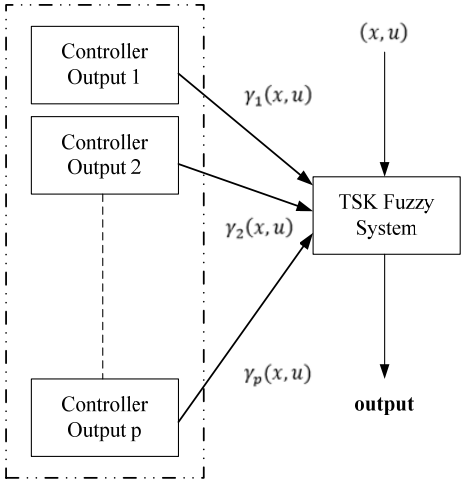

Fig. 4. General block diagram of the TS fuzzy controller.

3.1. Disturbance Rejection Strategy

First, disturbance rejection is followed by the feed-forward strategy. The compensating feed-forward term C_{ffi} is selected such that to eliminate the effect of disturbance in the system output. Let us consider the following disturbance compensation term.

$$u_{cri} = C_{ff\,i}\upsilon = [C_{ff\,1i}, C_{ff\,2i}]^T \upsilon \tag{13}$$

To compensate for the effect of disturbance on the output, the parameter C_{ffi} is designed to satisfy Eq. (14).

$$u_{cri} = C_{ff\,i}\upsilon + G_{\upsilon i}\upsilon = 0 \tag{14}$$

where $G_{pi} = [G_{p1i}, G_{p2i}]$ and $G_{\upsilon i}$ are the plant and disturbance transfer functions, respectively.

A possible solution for (14) is as follows:

$$C_{ff\,1i} = -G_{p1i}^{-1} G_{\upsilon i} \ \ and \ \ C_{ff\,2i} = 0$$

Remark 1: Since $C_{ff\,1i}$ is not a proper transfer function, we can select an adequate filter to deal with this problem.

3.2. Actuator Fault-Tolerant Controller Design

In practice, a common choice for the base-line controller is designed by LQR as $u_{base\,i} = -K_i\hat{x} + N_i\omega_{rref}$. The constant coefficient *N* is used to eliminate the tracking error. Since the system's states are not available, it is possible to formulate an observer for estimating the fault effects and the states of the system. To reduce the fault effects, a correction term is added as $u_{FTC} = E_f\hat{f}$. By addressing the actuator fault, we have D_f =0. The observer equations are as follows:

$$\begin{cases}\dot{\hat{x}} = (A_i - BK)\hat{x} + L(y - C\hat{x}) + BN_i\omega_{rref} \\ \dot{\hat{f}} = Q_i(y - C\hat{x})\end{cases} \tag{15}$$

By defining $e = x - \hat{x}$ as the estimation error and conducting some mathematical manipulations, we obtain

$$\begin{bmatrix}\dot{e} \\ \dot{\hat{f}}\end{bmatrix} = \left(\begin{bmatrix}A_i & BE_f \\ 0 & 0\end{bmatrix} - \begin{bmatrix}L_i \\ -Q_i\end{bmatrix}\begin{bmatrix}C & 0\end{bmatrix}\right)\begin{bmatrix}e \\ \hat{f}\end{bmatrix} + \begin{bmatrix}B_f \\ 0\end{bmatrix} f \tag{16}$$

Defining

$$\overline{E} = \begin{bmatrix}e^T & \hat{f}^T\end{bmatrix}^T,\ \overline{A}_i = \begin{bmatrix}A_i & BE_f \\ 0 & 0\end{bmatrix},\ \overline{B} = \begin{bmatrix}B_f \\ 0\end{bmatrix},$$

$$\overline{C} = \begin{bmatrix}C & 0\end{bmatrix} \text{ and } \overline{L}_i = \begin{bmatrix}L_i \\ -Q_i\end{bmatrix}$$

Thus, Eq. (16) can be simplified as follows:

$$\dot{\overline{E}} = (\overline{A}_i - \overline{L}_i\overline{C})\overline{E} + \overline{B}f \tag{17}$$

where E_f should be designed to eliminate the effect of faulty steady-state. It is assumed that E_f exists such that $BE_f + B_f = 0$. Next, we analyze the stability of the entire system.

Theorem 1: Let the state-space realization of the turbine be described by (9). The controller gain K is designed in such a way that $A_i - BK_i$ ($i = 1, \ldots, n$) is Hurwitz, and the gain of observer $\overline{L}_i$ satisfies the following LMIs for a positive scalar Γ :

$$\begin{bmatrix}O_1 & 0 & 0 & \ldots & 0 \\ 0 & O_2 & 0 & \ldots & 0 \\ \cdot & & & & \\ \cdot & & & & \\ \cdot & & & & \\ 0 & 0 & 0 & \ldots & O_n\end{bmatrix} < 0 \tag{18}$$

where

$$O_i = \begin{bmatrix}-2\Gamma^2 I & \overline{B}^T \\ B & \overline{A}_i - \overline{L}_i\overline{C} + \frac{1}{2}I\end{bmatrix} \qquad i = 1,2,\ldots,n \tag{19}$$

Then, the error $\overline{e}$ is the finite gain L_2 stable.

Proof: we construct the following Lyapunov function.

$$V = \frac{1}{2}\overline{E}^T\overline{E} \tag{20}$$

where

$$\dot{\overline{E}} = \sum_{i=1}^{n}\gamma_i(z(x,u))\left((\overline{A}_i - \overline{L}_i\overline{C})\overline{E} + \overline{B}f\right)$$

The time derivative of the Lyapunov function (20) is derived as follows:

$$\begin{aligned}\dot{V} &= \sum_{i=1}^{n}\gamma_i(z(x,u))\left(\frac{\partial V}{\partial \overline{E}}(\overline{A}_i - \overline{L}_i\overline{C})\overline{e} + \frac{\partial V}{\partial \overline{E}}\overline{B}_f\right) \\ &= \sum_{i=1}^{n}\gamma_i(z(x,u))\begin{pmatrix}-\frac{1}{2}\Gamma^2 \| f - \frac{1}{\Gamma^2}\overline{B}^T(\frac{\partial V}{\partial \overline{E}})^T \|_2^2 \\ +\frac{\partial V}{\partial \overline{E}}(\overline{A}_i - \overline{L}_i\overline{C})\overline{e} \\ +\frac{1}{2\Gamma^2}\frac{\partial V}{\partial \overline{E}}\overline{B}\,\overline{B}^T(\frac{\partial V}{\partial \overline{E}})^T\end{pmatrix}\end{aligned} \tag{21}$$

Considering Eqs. (18) and (19) and using Schur complement lemma, we have:

$$\overline{A}_i - \overline{L}_i\overline{C} + \frac{1}{2\Gamma^2}\overline{B}\,\overline{B}^T + \frac{1}{2}I \le 0, \qquad i = 1,2,\ldots,n \tag{22}$$

Using Eqs. (21) and (22), we obtain:

$$\dot{V} \le \sum_{i=1}^{n}\gamma_i(z(x,u))\begin{pmatrix}\frac{1}{2}\Gamma^2 \| u \|_2^2 - \frac{1}{2}\| y \|_2^2 \\ -\frac{1}{2}\Gamma^2 \| u - \frac{1}{\Gamma^2}\overline{B}^T(\frac{\partial V}{\partial \overline{E}})^T \|_2^2\end{pmatrix} \tag{23}$$

Now

$$\dot{V} \le \sum_{i=1}^{n}\gamma_i(z(x,u))\left(\frac{1}{2}\Gamma^2 \| u \|_2^2 - \frac{1}{2}\| y \|_2^2\right) \tag{24}$$

By integrating Eq. (24), it can be concluded that:

$$V(x(t)) - V(x(0)) \le n\begin{pmatrix}\frac{1}{2}\Gamma^2\int_0^t \| u(\tau) \|_2^2\, d\tau \\ -\frac{1}{2}\int_0^t \| y(\tau) \|_2^2\, d\tau\end{pmatrix} \tag{25}$$

Finally, by applying some mathematical manipulations, it is straightforward to see that the finite gain L_2 stability of error is proved as follows.

$$\| y \|_{L2} \le \Gamma \| u \|_{L2} + \sqrt{\frac{2V(x_0)}{n}} \tag{26}$$

3.3. Sensor Fault-Tolerant Controller Design

In this subsection, the baseline controller design and disturbance rejection structure are as the same as before. To design an FTC controller, it is necessary to estimate the fault. To achieve this goal, the sensor fault is estimated by the proposed observer. Hence, $B_f = 0$ due to the consideration of sensor fault. The control structure is the same as before, as depicted in Fig. 2. All of the true state values are estimated by the proposed observer, regardless of faults that occurred in the system. Therefore, the base line controller can work properly

without being affected by the fault. Eq. 12 shows the fuzzy control rule for disturbance rejection, FTC, and base line controller. The equivalent state-space representation is as follow:

$$\begin{cases} M\,\dot{Z}(t) = A_{s_i}\,Z(t) + B\,u(t) \\ y(t) = C_s\,Z(t) \end{cases} \tag{27}$$

where the state vector $ZT = [x^T f^T]$ and the matrices M, A_{si}, C_s are defined as:

$$M = [I, 0], \quad A_{s_i} = [A_{s_i}, 0], \quad C_s = [C, D_f] \tag{28}$$

By defining matrix W as

$$W = \begin{bmatrix} M \\ C_s \end{bmatrix} = \begin{bmatrix} I & 0 \\ C & D_f \end{bmatrix} \tag{29}$$

Assumption: We assume that the matrix D_f is a full column rank. Consequently, there exists left inverse of matrix W such that

$$[U\ V]\,W = I \tag{30}$$

where matrix $[U\ V]$ denotes the left inverse of W. The observer equations are

$$\begin{cases} \dot{\xi}(t) = (UA_{s_i} - L_i\,C_{s_i})\xi(t) \\ +(L + UA_{s_i}V - L_i\,C_{s_i}V)\,y(t) + B\,u(t) \\ \hat{Z}(t) = \xi(t) + V\,y(t) \end{cases} \tag{31}$$

It can be shown that sensor fault $f_2(t)$ can be estimated by:

$$D_f\ \hat{f}_2(t) = y(t) - C\,M\,Z(t) \tag{32}$$

in which u_{FTC} should be designed such that the effect of sensor fault on the output is tolerated. It can be seen that $u_{FTC}(t) = -N((y(t) - CMZ(t))$ removes the fault effect.

Table 1. Numerical value of a 1 MW wind turbine.

Turbine parameters	Description	Values	Dimension
K_s	Drivetrain stiffness parameter	1.566×10^6	N/m
$\overline{B}_s$	Drivetrain damping constant	3029.5	Nms/rad
$\overline{J}_r$	Rotor inertia	83×10^4	kg m^2
$\overline{J}_g$	Generator inertia	5.9	kg m^2
τ	Delay time constant for pitch dynamics	500×10^{-6}	s
ρ	Air density	1.225	kg m^3
R	Rotor radius	30.3	m

Theorem 2 For a given state-space realization of the turbine described by Eq. (9), the controller gain K is designed in such a way that $A_i - BK_i$ is Hurwitz for $i = 1, ..., n$. It is assumed that (UA_{si}, C_{si}) is observable and the observer gain L_i satisfies the following inequality for a symmetric positive definite matrix P:

$$(UA_{s_i} - L_i\,C_{s_i})^T P + P(UA_{s_i} - L_i\,C_{s_i}) < 0 \tag{33}$$

Proof By defining $e(t) = z(t) - \hat{z}(t)$ and constructing the Lyapunov function $V(t)=e^T(t)Pe(t)$, we have

$$\dot{e} = \dot{Z}(t) - \dot{\hat{Z}}(t) = \dot{Z}(t) - \dot{\xi}(t) + V\,\dot{y}(t) \tag{34}$$

$$= (I - V\,C_s)\,\dot{Z}(t) - \dot{\xi}(t) \tag{35}$$

By substituting $\dot{Z}$ and $\dot{\xi}$ in Eq. (34)

$$\begin{aligned} \dot{e} = U\,(A_{s_i}Z(t) + B\,u(t)) - ((UA_{s_i} - L_i\,C_{s_i})\xi(t) \\ +(L_i + UA_{s_i}V - L_i\,C_{s_i}V)\,y(t) + UB\,u(t)) \end{aligned} \tag{36}$$

After some manipulations, we have:

$$\dot{e}(t) = (UA_{s_i} - L_i\,C_{s_i})e(t) \tag{37}$$

Further, the time derivative of the Lyapunov function is calculated as follows:

$$\begin{aligned} V(t) = \dot{e}^T(t)\,Pe(t) + e^T(t)P\dot{e}(t) = \\ e^T(t)((UA_{s_i} - L_i\,C_{s_i})^T P + P(UA_{s_i} - L_i\,C_{s_i}))e(t) \end{aligned} \tag{38}$$

The stability proof can be verified by:

$$(UA_{s_i} - L_i\,C_{s_i})^T P + P(UA_{s_i} - L_i\,C_{s_i}) < 0 \tag{39}$$

4. SIMULATION RESULTS

Here, we illustrate and assess the capability of the proposed FTC by simulations. Figs. 5-15 provide the results of simulations in different conditions. Table. 1 tabulates the parameters of 1MW wind turbine used in the simulation. The proposed FTC-based controller is evaluated for a random variation of wind profile around the speed of 12 units, as shown in Fig. 5. The control design aims to achieve the rotor speed of $5^{rad}/_{s}$ without any fault in the FTC design. Based on the previous description, the wind speed plays a prominent role in the control design.

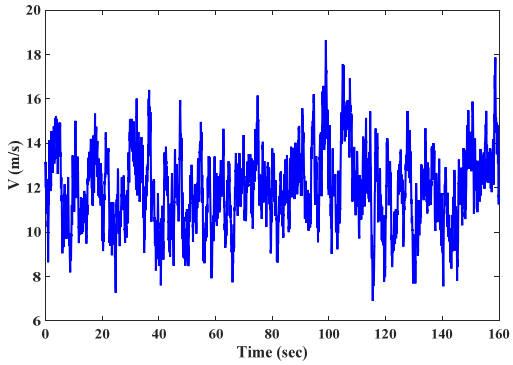

Fig. 5. The wind speed profile of 1 MW wind turbine.

The TS model should emulate WT dynamics. Therefore, relation (1) can be expressed by a set of TS fuzzy models as follows:

$$A_1=\begin{bmatrix} 0 & 1 & -1 & 0 \\ -\frac{\bar{K}_s}{\bar{J}_r} & -\frac{\bar{B}_s}{\bar{J}_r} & \frac{\bar{B}_s}{\bar{J}_r} & \frac{f_{1_{\min}}}{\bar{J}_r} \\ \frac{\bar{K}_s}{\bar{J}_g} & \frac{\bar{B}_s}{\bar{J}_g} & -\frac{(\bar{B}_s+\bar{B}_g)}{\bar{J}_g} & 0 \\ 0 & 0 & 0 & -\frac{1}{\tau} \end{bmatrix},\ W_1=\begin{bmatrix} 0 \\ \frac{f_{2_{\min}}}{J_r} \\ 0 \\ 0 \end{bmatrix}$$

$$A_2=A_1,\qquad W_2=\begin{bmatrix} 0 \\ \frac{f_{2_{\max}}}{J_r} \\ 0 \\ 0 \end{bmatrix}$$

$$A_3=\begin{bmatrix} 0 & 1 & -1 & 0 \\ -\frac{\bar{K}_s}{\bar{J}_r} & -\frac{\bar{B}_s}{\bar{J}_r} & \frac{\bar{B}_s}{\bar{J}_r} & \frac{f_{1_{\max}}}{\bar{J}_r} \\ \frac{\bar{K}_s}{\bar{J}_g} & \frac{\bar{B}_s}{\bar{J}_g} & -\frac{(\bar{B}_s+\bar{B}_g)}{\bar{J}_g} & 0 \\ 0 & 0 & 0 & \frac{1}{\tau} \end{bmatrix},\ W_3=W_1$$

$$A_4=A_3,\ W_4=W_2$$

$$B_i=\begin{bmatrix} 0 & 0 \\ 0 & 0 \\ 0 & \frac{1}{\bar{J}_g} \\ \frac{1}{\tau} & 0 \end{bmatrix},\quad i=1,\ldots,4 \tag{40}$$

We can easily obtain $f_{i\min}$ and $f_{i\max}$, i = 1, 2 in (Kamal et al., 2012). In the following, the actuator and sensor faults are estimated as the faults occur.

Remark 2: Four subsystems given in (40) can be considered based on the minimum and maximum values of parameters f and v. However, one can increase the number of subsystems of the overall system in terms of these parameters. In addition, using the FAST model of WT can enhance the validity of the proposed FTC design. How to deal with such limitation and validation will be investigated in our future work.

4.1. Actuator fault

The actuator fault is considered as a periodic signal. The gains of the base-line controller and observer are designed as:

$$K=\begin{bmatrix} -0.0336 & -0.4472 & 0.001 & 0.0489 \\ 0.001 & -0.002 & 0.002 & 0.001 \end{bmatrix} \tag{41}$$

$$L=\begin{bmatrix} 0.001 & 1.3497 & 1.3479 & -1 \end{bmatrix}$$

As shown in Fig. 6, the performance of the estimation actuator fault has good precision. Fig. 7 illustrates the estimated states $\hat{\theta}(s), \hat{\omega}_r, \hat{\omega}_g, \hat{\beta}$. Fig. 8 shows the system output and its reference. The control signals are depicted in Fig. 9, which are acceptable in practice.

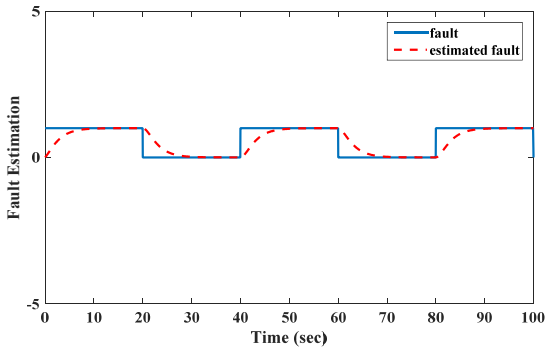

Fig. 6. Actual and estimated values of actuator fault.

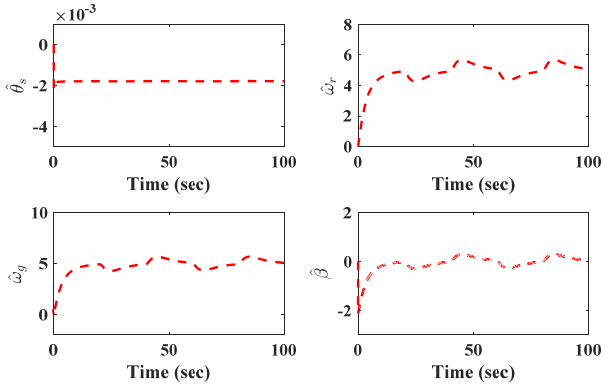

Fig. 7. Estimated values of shaft torsion angle, rotor angular velocity, generator angular velocity, and pitch angle in the presence of actuator fault states.

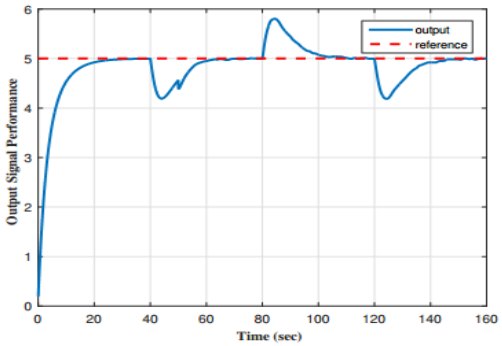

Fig. 8. Rotor angular velocity, as output, and its reference in the presence of actuator fault.

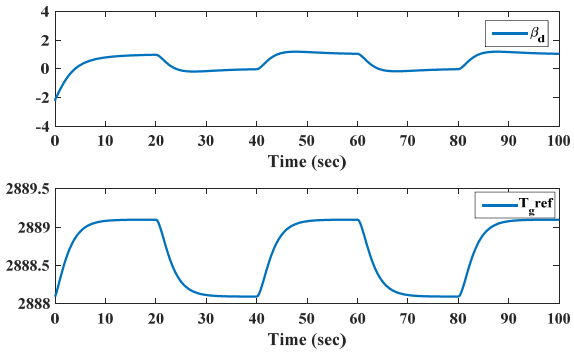

Fig. 9. The desired values of pitch angle and generator torque, as control signals, in the presence of actuator fault

4.2. Sensor fault

Similar to the previous subsection, a periodic signal is used for modelling a sensor fault. First, it is possible to obtain the gains of the controller and observer as follows:

$$K = \begin{bmatrix} -1.1838 & -4.4732 & 0.0012 & 2.3169 \\ 0.001 & -0.002 & 0.002 & 0.001 \end{bmatrix} \quad (42)$$

$$L = \begin{bmatrix} 0.0002 & 0.4145 \\ 0.5055 & 0.8605 \\ 0.3573 & 162.69 \\ 0.0001 & -0.0001 \\ 0.8628 & -0.5032 \end{bmatrix}$$

By using Eq. (42), the proposed FTC performance is examined under sensor fault. Fig. 10 demonstrates the successful achievement of the fault estimation. The responses of state estimations are depicted in Fig. 11. As shown in Fig. 12, the closed-loop system tolerates the faulty system, as the control goal is realized. Additionally, the behaviour of control inputs is represented by Fig. 13. As observed from Figs. 10-13, it can be concluded that the closed-loop FTC design has a satisfactory behaviour against sensor fault and the rotor speed tracking is provided during operation.

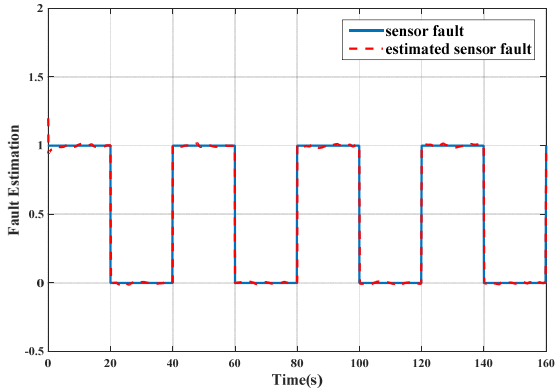

Fig. 10. Actual and estimated values of sensor fault.

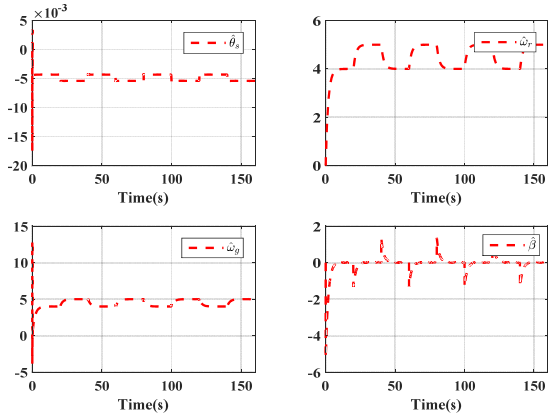

Fig. 11. Estimated values of shaft torsion angle, rotor angular velocity, generator angular velocity, and pitch angle in the presence of sensor fault

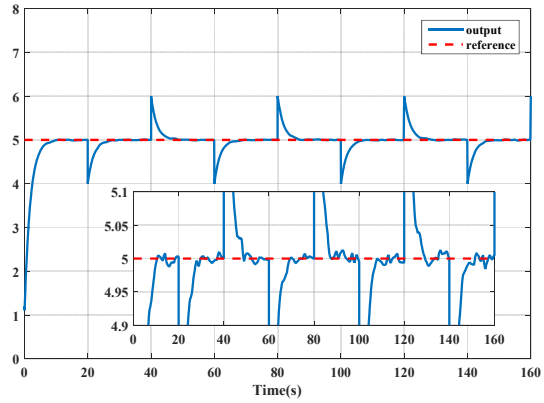

Fig. 12. Rotor angular velocity, as output, and its reference in the presence of sensor fault.

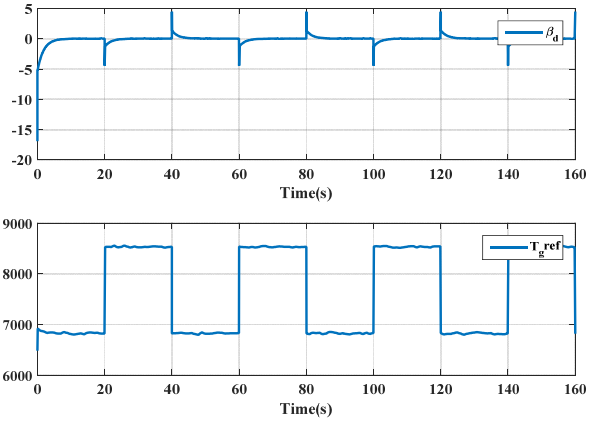

Fig. 13. The desired values of pitch angle and generator torque, as control signals, in the presence of sensor fault.

4.3. Comparison

To have a fair comparison, we adopted the robust LMI-based FTC design reported in (Bai et al., 2019) and redesigned it for the wind turbine system described by (1) in the presence of sensor fault. It is worth noting that one can easily rewrite the wind turbine's model in the following form:

$$\begin{aligned} \dot{x}(t) &= Ax(t) + Bu(t) + f(x,t) \\ &\quad + Bd(t) + g(t) \\ y(t) &= Cx(t) + f_s(t) \end{aligned} \quad (43)$$

Therefore, the FTC controller is expressed as follows:

$$\begin{aligned} u_{FTC}(t) &= -(\varepsilon + \bar{f_s} + \pi + \zeta(t) + \xi(t))\mathrm{sgn}(s_{\bar{x}}) \\ &\quad + K\hat{x}(t) \end{aligned} \quad (44)$$

in which

$$\begin{aligned} \zeta(t) &= \max\left\{\|\hat{\bar{d}}(t)\|, \|\hat{\underline{d}}(t)\|\right\} \\ \xi(t) &= \left\{\begin{matrix} \|(GB)^{-1}GL_{p1}\bar{C}\,\bar{x}(t)\| \\ +\|(GB)^{-1}GL_{p1}\bar{C}\,\hat{\bar{x}}(t)\| \end{matrix}\right\} \end{aligned} \quad (45)$$

Besides, the sliding mode observer addressed in (Bai et al., 2019) has been proposed as

$$\begin{aligned} S\dot{z}(t) &= \left(\bar{A} - \bar{L}_p\bar{C}\right)z(t) + \bar{B}u(t) + \bar{L}_s u_s(t) \\ &\quad + \bar{L}_p y(t) + \bar{F}f(\hat{x},t) \\ \hat{x}(t) &= z(t) + S^{-1}\bar{L}_N y(t) \end{aligned} \tag{46}$$

More details are given in (Bai et al., 2019). For summary, the definition of variables is omitted here (Please refer to the mentioned paper). Fig. 14 illustrates the tracking response of rotor speed based on the FTC-based design in (Bai et al., 2019). As shown in Figs. 12 and 14, it is inferred that the output tracking error of the proposed method is smaller than that of the method used in (Bai et al., 2019).

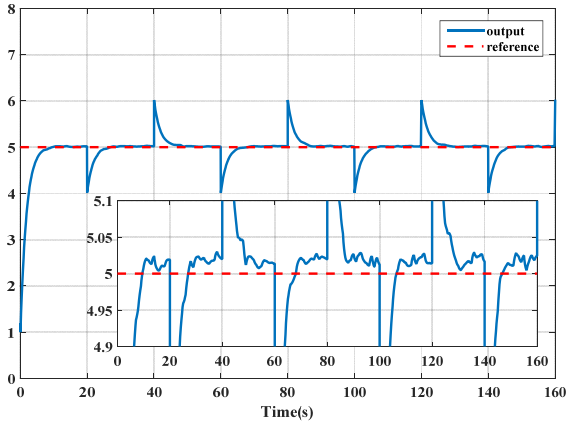

Fig. 14. Rotor angular velocity, as output, and its reference in comparison mode.

To show the superiority of the proposed FTC to the design addressed in (Bai et al., 2019), an effective criteria function is defined as follows:

$$\gamma_{\omega_r} = \frac{\sum_{i=1}^{Ns} e_{FTC_{\omega_r}}}{\sum_{i=1}^{Ns} e_{\omega_r}} \tag{47}$$

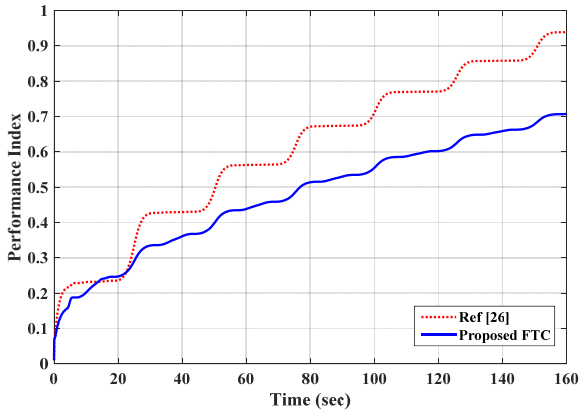

Fig. 15. Performance index of the proposed approach and method reported in [26].

in which e_{ω_r} represents the error of faulty rotor speed from the fault-free rotor speed (without applying an FTC), $e_{FTC_{\omega_r}}$ indicates the error of faulty rotor speed from the fault-free condition, in which FTC is activated in the control loop, and Ns shows the number of samples during the simulation. It can be deduced that $\gamma_{\omega_r} < 1$ shows an improvement in the FTC-based design. In other words, if the defined performance index of the proposed FTC becomes smaller than that of the comparison mode while it is lower than one, the proposed robust LMI-based design has a better reflection against fault. As shown in Fig. 15, γ_{ω_r} is equal to 0.705 in the proposed FTC method while it is 0.935 in the design-based approach (Bai et al., 2019). As a result, we can conclude that the proposed FTC is more appropriate to deal with sensor fault compared to the mentioned paper.

5. CONCLUSION

This paper sought to examine a new robust controller for a wind turbine in the form of LMIs, aiming to estimate and tolerate the actuator/sensor fault that occurred on the pitch system. The proposed FTC controller consisted of an LQR base-line controller, a disturbance rejection term, and a robust signal. The sufficient conditions were obtained to achieve the asymptotic stability of the entire system, including the FTC controller and the observer. Ultimately, numerical simulations highlight the capability of the proposed method for a 1 MW wind turbine system. Future works in this area is to design an adaptive fuzzy FTC for WT systems.

REFERENCES

Azizi, A., Nourisola, H., and Shoja-Majidabad, S. (2019). Fault tolerant control of wind turbines with an adaptive output feedback sliding mode controller. *Renewable Energy*, *135*, 55–65.

Badihi, H., Zhang, Y., and Hong, H. (2014). Fuzzy gain-scheduled active fault-tolerant control of a wind turbine. *Journal of the Franklin Institute*, *351*(7), 3677–3706.

Badihi, H., Zhang, Y., Pillay, P., and Rakheja, S. (2020). Fault-Tolerant Individual Pitch Control for Load Mitigation in Wind Turbines with Actuator Faults. *IEEE Transactions on Industrial Electronics*, *46*, 1–10.

Bai, L., Gao, Z., Qian, M., and Zhang, X. (2019). Sliding Mode Observer-Based FTC Strategy Design for Satellite Attitude Systems with Sensor Fault. *Proceedings of the 31st Chinese Control and Decision Conference, CCDC 2019*, 428–433.

Blesa, J., Rotondo, D., Puig, V., and Nejjari, F. (2014). FDI and FTC of wind turbines using the interval observer approach and virtual actuators/sensors. *Control Engineering Practice*, *24*(1), 138–155.

Burton, T., Jenkins, N., Sharpe, D., and Bossanyi, E. (2011). *Wind Energy Handbook*, Wiley.

Casau, P., Rosa, P., Tabatabaeipour, S. M., Silvestre, C., and Stoustrup, J. (2015). A set-valued approach to FDI and FTC of wind turbines. *IEEE Transactions on Control Systems Technology*, *23*(1), 245–263.

Ettouil, R., Chabir, K., and Abdelkrim, M. N. (2018). Synergetic fault-tolerant control for pitch control of wind turbine system. *Electrical Engineering*, *100*(4), 2527–2535.

Georg, S., and Schulte, H. (2014). Takagi-Sugeno Sliding

Mode Observer with a Weighted Switching Action and Application to Fault Diagnosis for Wind Turbines. *Advances in Intelligent Systems and Computing*, *230*, 41–52.

Ghanbarpour, K., Bayat, F., and Jalilvand, A. (2020). Wind turbines sustainable power generation subject to sensor faults: Observer-based MPC approach. *International Transactions on Electrical Energy Systems*, *30*(1), 11–13.

Habibi, H., Howard, I., and Simani, S. (2019). Reliability improvement of wind turbine power generation using model-based fault detection and fault tolerant control: A review. *Renewable Energy*, *135*, 877–896.

Haidegger, T., Kovács, L., Precup, R.E., Preitl, S., Benyó, B. and Benyó, Z. (2011). Cascade control for telerobotic systems serving space medicine. *IFAC Proceedings Volumes*, *44*(1), 3759-3764.

Haidegger, T., Kovács, L., Preitl, S., Precup, R.E., Benyo, B. and Benyo, Z. (2011). Controller design solutions for long distance telesurgical applications. *International Journal of Artificial Intelligence*, *6*(S11), .48-71.

Kamal, E., Aitouche, A., and Bayart, M. (2012). Fault tolerant control of wind energy conversion systems subject to sensor faults. *Ieee Transactions on Sustainable Energy*, *12*(2), 503–515.

Kühne, P., Pöschke, F., and Schulte, H. (2018). Fault estimation and fault-tolerant control of the FAST NREL 5-MW reference wind turbine using a proportional multi-integral observer. *International Journal of Adaptive Control and Signal Processing*, *32*(4), 568–585.

Li, J., Zhang, D., and Wang, Z. (2020). Novel MPC-Based Fault Tolerant Tracking Control Against Sensor Faults. *Asian Journal of Control*, *22*(2), 841–854.

Nourdine, S., Camblong, H., Vechiu, I., and Tapia, G. (2010). Comparison of wind turbine LQG controllers using Individual Pitch Control to alleviate fatigue loads. *18th Mediterranean Conference on Control and Automation, MED'10 - Conference Proceedings*, 1591–1596.

Obe, O. and Dumitrache, I. (2012). Adaptive neuro-fuzzy controler with genetic training for mobile robot control. *International Journal of Computers Communications & Control*, *7*(1), 135-146.

Odgaard, P. F., and Johnson, K. E. (2013). Wind turbine fault detection and fault tolerant control - An enhanced benchmark challenge. *Proceedings of the American Control Conference*, 4447–4452.

Odgaard, P. F., Stoustrup, J., and Kinnaert, M. (2013). Fault-tolerant control of wind turbines: A benchmark model. *IEEE Transactions on Control Systems Technology*, *21*(4), 1168–1182.

Saha, C., and Singh, A. K. (2019). A Review Article on Fault-Tolerant Control (FTC) and Fault Detection Isolation (FDI) Schemes of Wind Turbine. In *Proceeding of the second international conference on microelectronics, computing & communication systems*, 476, 87–95.

Schulte, H., and Gauterin, E. (2015). Fault-tolerant control of wind turbines with hydrostatic transmission using Takagi-Sugeno and sliding mode techniques. *Annual Reviews in Control*, *40*, 82–92.

Shi, F., and Patton, R. (2015). An active fault tolerant control approach to an offshore wind turbine model. *Renewable Energy*, *75*, 788–798.

Simani, S., and Castaldi, P. (2014). Active actuator fault-tolerant control of a wind turbine benchmark model S. *International Journal of Robust and Nonlinear Control*, *24*, 1283–1303.

Sloth, C., Esbensen, T., and Stoustrup, J. (2011). Robust and fault-tolerant linear parameter-varying control of wind turbines. *Mechatronics*, *21*(4), 645–659.

Soltani, M. N., Knudsen, T., Svenstrup, M., Wisniewski, R., Brath, P., Ortega, R., and Johnson, K. (2013). Estimation of rotor effective wind speed: A comparison. *IEEE Transactions on Control Systems Technology*, *21*(4), 1155–1167.

Taher, S. A., Farshadnia, M., and Mozdianfard, M. R. (2013). Optimal gain scheduling controller design of a pitch-controlled VS-WECS using de optimization algorithm. *Applied Soft Computing Journal*, *13*(5), 2215–2223.

Tanaka, K., and Wang, H. O. (2003). Takagi-Sugeno Fuzzy Model and Parallel Distributed Compensation, *Fuzzy control systems design and analysis: A linear matrix inequality approach*, Chapter 2, Wiley.

Xiahou, K. S., Liu, Y., Li, M. S., and Wu, Q. H. (2020). Sensor fault-tolerant control of DFIG based wind energy conversion systems. *International Journal of Electrical Power and Energy Systems*, *117*(September 2019).